Reliable Computing (2006) **12:** 451–470
DOI: 10.1007/s11155-006-9014-5

Uncertainty in Thermal Basin Modeling: An Interval Finite Element Approach

SEBASTIÃO C. PEREIRA
PETROBRAS R&D Center, Rua Jequitibá 950, Cidade Universitária, Ilha do Fundão, Rio de Janeiro, RJ 21941–598, Brazil, e-mail: sebastiaop@petrobras.com.br

ULISSES T. MELLO
IBM Thomas J. Watson Research Center, P.O. Box 218, Yorktown Heights, NY 10598, USA, e-mail: ulisses@watson.ibm.com

NELSON F. F. EBECKEN
Federal University of Rio de Janeiro, P.O. Box 68506, Rio de Janeiro, RJ 21945–970, Brazil, e-mail: nelson@ntt.ufrj.br

and

RAFI L. MUHANNA
Center for Reliable Engineering Computing (REC), School of Civil & Environmental Engineering, Georgia Institute of Technology, 210 Technology Circle, Savannah, GA 31407–3038, USA, e-mail: rafi.muhanna@gtsav.gatech.edu

(Received: 22 November 2004; accepted: 25 August 2005)

Abstract. Uncertainty assessment in basin modeling and reservoir characterization is traditionally treated by geostatistical methods which are normally based on stochastic probabilistic approaches. In this paper, we present an alternative approach which is based on interval arithmetic. Here, we discuss a finite element formulation which uses interval numbers rather than real numbers to solve the transient heat conduction in sedimentary basins. For this purpose, a novel formulation was developed to deal with both the special interval arithmetic properties and the transient term in the differential Equation governing heat transfer. In this formulation, the "stiffness" matrix resulting from the discretization of the heat conduction equation is assembled with an element-by-element technique in which the elements are globally independent and the continuity is enforced by Lagrange multipliers. This formulation is an alternative to traditional Monte Carlo method, where it is necessary to run a simulation several times to estimate the uncertainty in the results. We have applied the newly developed techniques to a one-dimensional thermal basin simulation to assess their potential and limitations. We also compared the quality of our formulation with other solution methods for interval linear systems of equations.

1. Introduction

Determinist numerical simulations are normally used to predict the behavior of geological systems. The predicted behavior or performance is normally used for risk assessment. A well known limitation of determinist simulations is that they provide a single set of results that do not convey information about the uncertainty associated with input parameters or coefficients. To overcome this limitation, uncertainty

assessment is typically coupled with stochastic probabilistic approaches in which the input simulation parameter set is stochastically defined and multiple simulations are executed to estimate the uncertainty associated with a probabilistic distribution of the input parameter space. While effective, this approach is rather expensive computationally. In addition, in deterministic numerical simulations, such as the traditional finite element approach, all the parameters are assumed to be precisely known. However, frequently in basin modeling this is not the case, since imprecise or fuzzy information may be present in the geometry, age, and material properties of the basin. Stochastic or probabilistic approaches have been developed to account for these kinds of uncertainties. However, in these approaches material properties are normally treated as random variables despite the fact that some geological processes are not controlled by random phenomena. In this work, we present an alternative to the stochastic probabilistic approaches which is based on interval mathematics to assess uncertainty. We have applied the newly developed techniques to a one-dimensional thermal basin simulation to assess their potential and limitations.

Interval mathematics is a generalization in which interval numbers replace real, or exact crisp, numbers, interval arithmetic replaces real arithmetic and interval analysis replace real analysis [3]. Fuzzy numbers can be represented by confidence intervals and calculations can be performed through interval mathematics. For a introduction to interval and fuzzy arithmetic we recommend reading [5], [12], and [25]. Appendix A summarizes the most common interval operations and their properties. To be unconditionally stable, the numerical solution of partial differential equations (PDEs), governing the heat and fluid transfer in porous media, normally requires that the time discretization is implicit. This stable solution leads to a set of simultaneous linear system of equations. When fuzzy numbers are used to represent material properties, such as thermal conductivity, the description of the resulting linear system is no longer crisp, but is ambiguous or imprecise. This requires the linear system to be solved using a non-classic approach and unfortunately, there are very few efficient methods described in the literature to solve these systems. It is noteworthy that the solution of interval linear system is combinatorial in nature and the result is a convex hull bounding all possible solutions for the imprecise input system. The combinatorial method is the most accurate method for solving interval systems of equations, generally they are inner bounds. In this method, the system of equation is solved for all combinations of interval numbers using their upper and lower bounds. Needless to say, the combinatorial method is extremely expensive and cannot solve large systems. However, it can be used to evaluate the accuracy of other methods for small systems. A method is said to overestimate the results when they are larger than the hull estimated by the combinatorial method.

The classic approaches to solve interval linear systems, such as Gaussian elimination, fail to solve interval systems because of some special properties of interval arithmetic, such as the subcancel property, in which one number minus itself is not zero, and one number divided by itself is not the unit. These properties require extensive modifications to the algorithms to solve the systems. In addition, the

overestimation induced by variable repetition in a mathematical expression makes it especially difficult to deal with interval numbers. In the literature, several papers have described methods to solve interval linear systems of equations. For example, Neumaier [25] proposed a preconditioning variation to Gauss Elimination and the Gauss Seidel Method. Unfortunately, these techniques generate overestimation in the solution and they also fail to solve both large problems and systems with large interval widths. Rao [29] discussed an optimization method using algorithm Powell to solve interval linear systems. This method is very expensive and frequently generates results in which the range is too tight, underestimating the results. Recently Muhanna [18] presented an interval-based finite element formulation which makes use of an Element-by-Element (EBE) technique to calculate the solution of steady-state problems in mechanics. This avoids most sources of overestimations and computes a very sharp solution hull. In this paper, we extend the EBE technique to handle time dependent problems. In addition, we briefly describe a C++ library that we implemented with the combinatorial, preconditioned Gauss elimination, Gauss Seidel, and the Powell methods to solve interval linear systems of equations.

Throughout this paper, boldface will denote intervals, lower case will denote scalar quantities, and upper case will denote vectors and matrices. Underscores will denote lower bounds of intervals and overscores will denote upper bounds of intervals.

2. Heat Transfer in Sedimentary Basins

To illustrate the interval-based uncertainty analysis in basin modeling, we discuss the effect of uncertainty in the thermal conductivity of rocks on the predicted temperature evolution of a given basin. The thermal conductivity of sedimentary rocks is a material property which is well known to vary largely in nature and the impact of its variation can be evaluated with interval mathematics. Thermal conductivity is a key parameter in the partial differential equation that governs the heat transfer in compacting porous sediments [8]:

$$\left[\frac{\varphi}{(1-\varphi)}\rho_f c_f + \rho_s c_s\right]\frac{\partial T}{\partial t} = \frac{\partial}{\partial Z}\left[\alpha_b(1-\varphi)\frac{\partial T}{\partial Z}\right] - \rho_f c_f q_f \frac{\partial T}{\partial Z} + \frac{Q_h}{(1-\varphi)}, \quad (2.1)$$

where:

φ = sediment porosity,
ρ_f = pore fluid density,
c_f = pore fluid specific heat,
ρ_s = solid grain density,
c_s = solid grain specific heat,
T = temperature,
t = time,

α_b = bulk (solid + fluid) thermal conductivity of sediments,

$Z = \int_{z1}^{z2} (1 - \varphi)\, dz$ = fully compacted depth,

q_f = darcian fluid velocity,

Q_h = heat source/sink.

Equation (2.1) describes the transfer of heat within the sediments via diffusion and advection processes. The bracketed term in the left-hand side of (2.1) is the sediment bulk heat capacity. The first term in the right hand side describes the conduction of heat, the second term represents the advection due to fluid carriage of heat and the final term accounts for the heat gained or lost sources or sinks. The respective essential and natural boundary conditions used to solve (2.1) are:

$$T(S_z) = T_{\text{surf}}(t), \tag{2.2}$$

$$\alpha_b(1 - \varphi)\frac{\partial T}{\partial Z}\bigg|_{z=0} = Q(t), \tag{2.3}$$

where T_{surf} is the temperature at the interface water-sediment and $Q(t)$ is the basal heat flux entering the basin. This heat flux can be calculated by the degree of crustal and lithospheric mantle thinning as described by McKenzie [7]:

$$Q(t) = \frac{\alpha_a T_m}{a}\left[1 + \frac{\beta}{\pi}\sum_{n=1}^{\infty} \sin\left(\frac{n\pi}{\beta}\right) \exp\left(\frac{-n^2\pi^2\lambda t}{a^2}\right)\right], \tag{2.4}$$

where:

α_a = lithosphere thermal conductivity,

T_m = mantle temperature,

a = lithosphere thickness,

λ = $(k_a / \rho c)$ = thermal diffusivity,

c = specific heat,

τ = $(a^2 / \pi^2 k)$ = thermal decay,

β = lithosphere extension factor.

For deterministic solutions, we have used the data displayed in Tables 1 and 2. Table 1 shows the physical properties for typical sediments and Table 2 presents typical lithospheric parameters.

3. Traditional Finite Element Formulation for the Transient Heat Conduction

Before we discuss the interval finite element formulation, we briefly review the traditional deterministic Galerkin finite element formulation for solving (2.1). By

Table 1. Physical properties of selected lithologies, where: φ_0 = surface porosity; b = porosity decay coefficient; ρ = density; α = thermal conductivity; C = heat capacity.

Lithology	φ_0	b (1/km)	ρ (g/cm^3)	α (W/m ^{o}C)	C (J/kg ^{o}C)
Shale	63.0	0.58	2.68	1.5	950.0
Silt	56.0	0.39	2.68	2.0	860.0
Sandstone	50.0	0.50	2.65	3.0	750.0
Limestone	60.0	0.44	2.72	2.5	860.0
Chalk	70.0	0.71	2.67	3.5	800.0
Salt	0.05	0.005	2.20	5.5	854.0
Basalt	5.00	0.0	2.85	2.0	775.0

Table 2. Lithosphere properties.

Thermal diffusivity	0.008	(m^2/s)
Thermal expansion coefficient	0.000034	(1/°C)
Crustal thickness	31200.0	(m)
Lithosphere thickness	125000.0	(m)
Temperature at the lithosphere base	1333.0	(°C)
Mantle density	3330	(kg/m^3)
Crustal density	2800	(kg/m^3)
Constant basement heat flow	41.84	(mW/m^2)

neglecting the advection term in (2.1), this equation then describes a general diffusion problem which can be stated as an initial-boundary value problem (IBV). It can be expressed in a general form by the following differential equation [1]:

$$\mu(x)\frac{\partial U(x,t)}{\partial t} - \frac{\partial}{\partial x}\left(\alpha(x)\frac{\partial U(x,t)}{\partial x}\right) = f(x,t). \tag{3.1}$$

When (3.1) is applied to heat conduction, its symbols represent:

$$\begin{aligned} U(x,t) = T(x,t) &= \text{temperature},\\ \mu(x) = \rho(x)c(x) &= \text{heat storage},\\ f(x,t) = Q(x,t) &= \text{heat source},\\ \rho(x) &= \text{density},\\ c(x) &= \text{specific heat}. \end{aligned}$$

IBV problems consists of finding $U = U(x)$ satisfying (3.1) $\forall x \in \Omega$ and the prescribed boundary conditions (BCs) which are assumed take the form:

$$U(x) = g(x) \qquad \forall x \in \Gamma_g, \tag{3.2}$$

$$\alpha\frac{\partial U}{\partial x} = h(x) \qquad \forall x \in \Gamma_h, \tag{3.3}$$

where Ω is the domain and Γ the boundary, g and h are given functions, g is the essential, or Dirichlet BC, and h is the natural, or Newman BC.

Approximating $U = Na$ and solving (3.1) by the Galerkin method in space and the fully implicit method in time using the backward finite difference [1, p. 459] results into the following element equations:

$$[k_{\text{eff}}]\{a\}_n = \{f_{\text{eff}}\}, \tag{3.4}$$

where:

$$[k_{\text{eff}}] = \frac{1}{\Delta t_n}[c] + [k], \tag{3.5}$$

$$\{f_{\text{eff}}\} = \{f\}_n + \left(\frac{1}{\Delta t_n}[c]\right)\{a\}_{n-1}, \tag{3.6}$$

$$\begin{aligned} \Delta t_n &= \text{time step } n, \\ \{a\}_{n-1} &= \text{solution for the time-step } n-1, \\ N &= \text{shape functions.} \end{aligned}$$

The coefficients of the element "stiffness" (k) and accumulation (c) matrices are given by:

$$k = \begin{bmatrix} \frac{\alpha}{L} & -\frac{\alpha}{L} \\ -\frac{\alpha}{L} & \frac{\alpha}{L} \end{bmatrix}, \qquad c = \begin{bmatrix} \frac{1}{3}\mu L & \frac{1}{6}\mu L \\ \frac{1}{6}\mu L & \frac{1}{3}\mu L \end{bmatrix}, \tag{3.7}$$

where L is the length of 1D finite element. The accumulation matrix represents the element heat storage capacity, μ. For the global solution of the IBV problem, the elements are assembled in a global stiffness K_{eff} and in a global F_{eff} vector. Then a linear system of equations is solved for the primary variable a:

$$[K_{\text{eff}}]\{a\}_n = \{F_{\text{eff}}\}, \tag{3.8}$$

$$[K_{\text{eff}}] = \mathop{\mathbf{A}}_{e=1}^{nel} k_{\text{eff}},$$

$$\{F_{\text{eff}}\} = \mathop{\mathbf{A}}_{e=1}^{nel} f_{\text{eff}},$$

where symbol **A** represents the assembly operation.

4. The Element-by-Element (EBE) Formulation with Element Overlap

A straightforward way to transform the traditional finite element formulation into a interval finite element formulation is to replace the real "stiffness" matrix by an interval, or fuzzy, stiffness matrix and solve the resulting interval linear system. Unfortunately, the direct solution of this linear system of equations can produce overestimated results and arithmetic operation problems [6]. This occurs due to

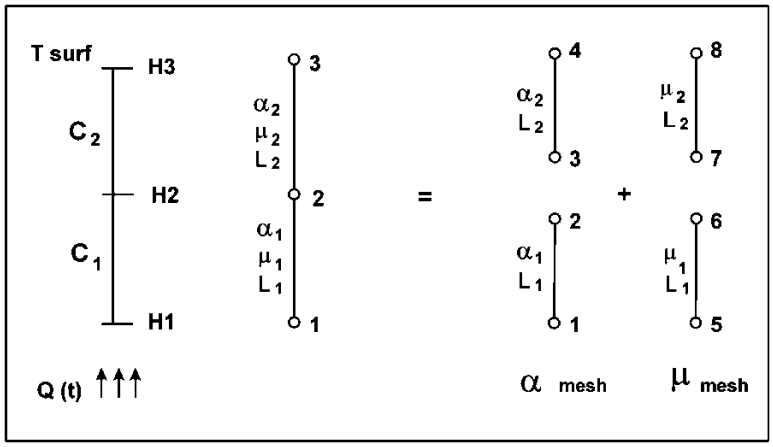

Figure 1. EBE scheme for a mesh with 2 elements. The nodes are split and renumbered producing 4 overlapping elements.

the large number of arithmetic operations and the width of the intervals numbers during the solution process. Muhanna [18] proposed an EBE finite element method for steady-state problems that avoids a great number of these operations. In his method, the assembly operation is modified by keeping the elements effectively disconnected and enforcing continuity in the mesh by using Lagrange constraints. Using this approach, the stiffness matrix can be factored in to two matrices: one interval diagonal matrix and another real banded matrix. The inversion of these matrices is done separately and involves very few interval arithmetic operations because the inversion of the diagonal matrix requires a single interval division per row. In spite of this advance, this method is not directly applied to transient problems in which the stiffness matrix has the contribution of the heat capacity term (C matrix). In this case, the resulting stiffness matrix cannot be factored using the same algorithm that was described for the steady-state case.

In the sequence, we discuss a new formulation to extend the EBE formulation to solve interval transient heat conduction problems. The goal of this formulation is the same as the steady-state formulation described previously, that is, to factor the global stiffness matrix into two matrices, one interval diagonal and another banded real, to reduce the number of arithmetic operations involving interval numbers during the solution of the linear system.

Figure 1 illustrates the EBE formulation using a one-dimensional thermal basin modeling example. In this example, there are three stratigraphic horizons (H_i, $i = 1\ldots3$) and two layers (C_i, $i = 1\ldots2$) represented by the traditional finite element mesh with three nodes (horizons) and two elements (layers). The heat flux is specified (natural condition) at the bottom ($Q(t)$) and the surface temperature is specified (essential boundary) at the top (T_{surf}). Each layer i, has its own physical properties: conductivity (α_i), heat capacity (μ_i), and thickness (L_i).

The overlapping elements are on the right (Figure 1). There is essentially one mesh for the conductivity (α mesh) overlapping with another one for the heat capacity (μ mesh). The thermal conductivity and the heat capacity are interval numbers represented by $\boldsymbol{\alpha} = [\underline{\alpha}, \overline{\alpha}]$ and the $\boldsymbol{\mu} = [\underline{\mu}, \overline{\mu}]$. After the mesh split, the nodes are duplicated, node 1 becomes 1 and 5; node 2 becomes 2, 3, 6, 7; and node 3 becomes 4, 8. The mesh compatibility, or the resulting continuity, has to be enforced and thus constraining equations must be satisfied: $T_1 = T_5$; $T_2 = T_3 = T_6 = T_7$; $T_4 = T_8$, where T is temperature.

The global linear system of equations with the node compatibilities using the EBE formulation with overlap for this mesh is:

$$\begin{bmatrix}
\frac{\boldsymbol{\alpha}_1}{L_1} & -\frac{\boldsymbol{\alpha}_1}{L_1} & & & & & & & 1 & 0 & 0 & 0 & 0 \\
-\frac{\boldsymbol{\alpha}_1}{L_1} & \frac{\boldsymbol{\alpha}_1}{L_1} & & & & & & & 0 & 1 & 1 & 1 & 0 \\
 & & \frac{\boldsymbol{\alpha}_2}{L_2} & -\frac{\boldsymbol{\alpha}_2}{L_2} & & 0 & & & 0 & -1 & 0 & 0 & 0 \\
 & & -\frac{\boldsymbol{\alpha}_2}{L_2} & \frac{\boldsymbol{\alpha}_2}{L_2} & & & & & 0 & 0 & 0 & 0 & 1 \\
 & & & & \frac{\boldsymbol{\mu}_1 L_1}{3\Delta t} & \frac{\boldsymbol{\mu}_1 L_1}{6\Delta t} & & & -1 & 0 & 0 & 0 & 0 \\
 & & 0 & & \frac{\boldsymbol{\mu}_1 L_1}{6\Delta t} & \frac{\boldsymbol{\mu}_1 L_1}{3\Delta t} & & & 0 & 0 & -1 & 0 & 0 \\
 & & & & & & \frac{\boldsymbol{\mu}_2 L_2}{3\Delta t} & \frac{\boldsymbol{\mu}_2 L_2}{6\Delta t} & 0 & 0 & 0 & -1 & 0 \\
 & & & & & & \frac{\boldsymbol{\mu}_2 L_2}{6\Delta t} & \frac{\boldsymbol{\mu}_2 L_2}{3\Delta t} & 0 & 0 & 0 & 0 & -1 \\
1 & 0 & 0 & 0 & -1 & 0 & 0 & 0 & 0 & 0 & 0 & 0 & 0 \\
0 & 1 & -1 & 0 & 0 & 0 & 0 & 0 & 0 & 0 & 0 & 0 & 0 \\
0 & 1 & 0 & 0 & 0 & -1 & 0 & 0 & 0 & 0 & 0 & 0 & 0 \\
0 & 1 & 0 & 0 & 0 & 0 & -1 & 0 & 0 & 0 & 0 & 0 & 0 \\
0 & 0 & 0 & 1 & 0 & 0 & 0 & -1 & 0 & 0 & 0 & 0 & 0
\end{bmatrix} \cdot \begin{Bmatrix} \boldsymbol{T}_1 \\ \boldsymbol{T}_2 \\ \boldsymbol{T}_3 \\ \boldsymbol{T}_4 \\ \boldsymbol{T}_5 \\ \boldsymbol{T}_6 \\ \boldsymbol{T}_7 \\ \boldsymbol{T}_8 \\ \boldsymbol{\lambda}_1 \\ \boldsymbol{\lambda}_2 \\ \boldsymbol{\lambda}_3 \\ \boldsymbol{\lambda}_4 \\ \boldsymbol{\lambda}_5 \end{Bmatrix} = \begin{Bmatrix} \boldsymbol{P}_1 \\ \boldsymbol{P}_2 \\ \boldsymbol{P}_3 \\ \boldsymbol{P}_4 \\ \boldsymbol{P}_5 \\ \boldsymbol{P}_6 \\ \boldsymbol{P}_7 \\ \boldsymbol{P}_8 \\ 0 \\ 0 \\ 0 \\ 0 \\ 0 \end{Bmatrix} \tag{4.1}$$

or more compactly:

$$\begin{bmatrix} \boldsymbol{K} & C^T \\ C & 0 \end{bmatrix} \begin{Bmatrix} \boldsymbol{T} \\ \boldsymbol{\lambda} \end{Bmatrix} = \begin{Bmatrix} \boldsymbol{P} \\ 0 \end{Bmatrix}, \tag{4.2}$$

where $\boldsymbol{K}$ is the stiffness matrix, C is the compatibility node matrix, $\boldsymbol{T}$ the unknown temperature, $\boldsymbol{\lambda}$ the vector of Lagrange multipliers, and $\boldsymbol{P}$ is the heat source. The first two blocks in the diagonal of the stiffness matrix in (4.1) are from the thermal conductivity mesh. The third and fourth blocks are from to heat capacity elements. The 0, 1, and -1 coefficients are from the constraining equations used to enforce the node compatibilities. The linear system of equation above can also be written as:

$$\boldsymbol{K}\boldsymbol{T} + C^T\boldsymbol{\lambda} = \boldsymbol{P}, \tag{4.3}$$

$$C\boldsymbol{T} = 0. \tag{4.4}$$

The stiffness matrix ($\boldsymbol{K}$) can be written as the product of two matrices:

$$\boldsymbol{K} = \boldsymbol{D}S, \tag{4.5}$$

where $\boldsymbol{D}$ is an interval diagonal matrix and S is a banded real matrix:

$$\boldsymbol{D} = \begin{pmatrix} \frac{\boldsymbol{\alpha}_1}{L_1} & & & & & & & & \\ & \frac{\boldsymbol{\alpha}_1}{L_1} & & & & & & & \\ & & \frac{\boldsymbol{\alpha}_2}{L_2} & & & 0 & & & \\ & & & \frac{\boldsymbol{\alpha}_2}{L_2} & & & & & \\ & & & & \frac{\boldsymbol{\mu}_1 L_1}{\Delta t} & & & & \\ & & 0 & & & \frac{\boldsymbol{\mu}_1 L_1}{\Delta t} & & & \\ & & & & & & \frac{\boldsymbol{\mu}_2 L_2}{\Delta t} & & \\ & & & & & & & \frac{\boldsymbol{\mu}_2 L_2}{\Delta t} & \end{pmatrix}, \tag{4.6}$$

$$S = \begin{pmatrix} 1 & -1 & & & & & & \\ -1 & 1 & & & & 0 & & \\ & & 1 & -1 & & & & \\ & & -1 & 1 & & & & \\ & & & & \frac{1}{3} & \frac{1}{6} & & \\ & & & & \frac{1}{6} & \frac{1}{3} & & \\ & 0 & & & & & \frac{1}{3} & \frac{1}{6} \\ & & & & & & \frac{1}{6} & \frac{1}{3} \end{pmatrix}. \tag{4.7}$$

Since the diagonal matrix $\boldsymbol{D}$ has the interval numbers ($\boldsymbol{\alpha}$ and $\boldsymbol{\mu}$), its inverse is obtained trivially. The S matrix is block diagonal and singular (the second line equals to the first multiplied by -1) and, thus, cannot be directly inverted. Substituting (4.5) in (4.3) results in:

$$\boldsymbol{DST} = \boldsymbol{P} - C^T \boldsymbol{\lambda}. \tag{4.8}$$

Multiplying (4.4) by $\boldsymbol{DC}^T$, and adding the result to (4.8), after some algebraic operations we obtain:

$$\boldsymbol{D}(\boldsymbol{ST} + C^T C\boldsymbol{T}) = \boldsymbol{P} - C^T \boldsymbol{\lambda}. \tag{4.9}$$

If we define $Q = C^T C$ and $R = S + Q$ we have:

$$\boldsymbol{DRT} = \boldsymbol{P} - C^T \boldsymbol{\lambda}. \tag{4.10}$$

Finally, the temperature solution vector can be obtained from (4.10) by:

$$\boldsymbol{T} = R^{-1}\boldsymbol{D}^{-1}(\boldsymbol{P} - C^T \boldsymbol{\lambda}). \tag{4.11}$$

This equation can be further simplified by defining the vector:

$$\boldsymbol{V} = (\boldsymbol{P} - C^T \boldsymbol{\lambda}) = (v_1, v_2, v_3, v_4, v_5, v_6, v_7, v_8)^T, \tag{4.12}$$

then (4.11) becomes:

$$\boldsymbol{T} = R^{-1} \boldsymbol{M} \boldsymbol{\delta}, \tag{4.13}$$

where:

$$\boldsymbol{M} = \begin{bmatrix} v_1 & 0 & 0 & 0 \\ v_2 & 0 & 0 & 0 \\ 0 & v_3 & 0 & 0 \\ 0 & v_4 & 0 & 0 \\ 0 & 0 & v_5 & 0 \\ 0 & 0 & v_6 & 0 \\ 0 & 0 & 0 & v_7 \\ 0 & 0 & 0 & v_8 \\ 1 & 0 & 0 & 0 \end{bmatrix} \quad \text{and} \quad \boldsymbol{\delta} = \begin{Bmatrix} \dfrac{L_1}{\alpha_1} \\ \dfrac{L_2}{\alpha_2} \\ \dfrac{\Delta t}{\mu_1 L_1} \\ \dfrac{\Delta t}{\mu_2 L_2} \end{Bmatrix}. \tag{4.14}$$

The matrix $\boldsymbol{M}$ has dimensions (4 × number of elements) × (2 × number of elements) and the vector $\boldsymbol{\delta}$ has dimensions 2 × number of elements. The rows of the vector $\boldsymbol{\delta}$ are essentially the diagonal values of $\boldsymbol{D}^{-1}$. Because the interval numbers occur only once in this vector, we avoid interval operation repetition with the same number. The matrix sizes are twice as large as the EBE for steady-state formulation because of the mesh duplication. This is the main cost of using this technique to reduce the number of interval operations.

5. Details of the Implementation

We have implemented a new library to solve interval linear systems of equations using Object-Oriented (OO) technologies in C++. By making use of templates and traits techniques we have been able to develop a library that can solve a linear systems of equations for distinct types of numbers such as real, interval and fuzzy, using the same implementation. This library can also handle different matrix storage structures such as dense, banded, and tridiagonal. In this library, we have implemented the following methods: (1) preconditioned Gauss-Seidel [6]; (2) Preconditioned Gaussian elimination [6]; (3) optimization using Powell's method [28]; and (4) the combinatorial method [16]. Figure 2 is a graphical representation of a fuzzy linear system of equations with triangle numbers. It shows that a fuzzy system can be solved by α-cuts planes of interval linear system of equations.

In Figure 3, we display the class derivation scheme for numbers and matrices, as well as the main algorithm classes for the solution of linear systems. Following the OO approach, each class number is responsible for its operations (addition, subtraction, multiplication, division, absolute value, etc). This data encapsulation approach is also applied to each matrix class which is responsible for its own

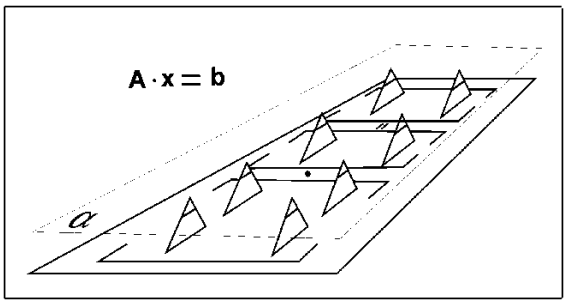

Figure 2. Fuzzy linear system of equations.

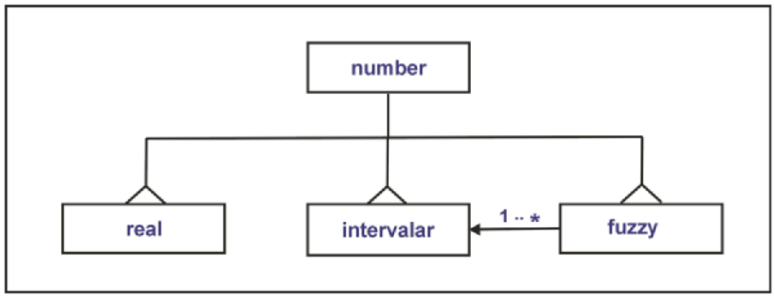

Figure 3. Derivation class for number types.

matrix operations (LU decomposition, vector multiply, inverse, determinant, rank, etc). We used the classes implemented by Deodato [2] for interval and fuzzy number operations. In his implementation, the fuzzy number is subdivided in α-cuts confidence intervals. We made extensive use of operator overloading, inlining, and templates in our implementation.

By using templates and the generic programming approach [11], we were able to have a single implementation for the solution of the system ($\boldsymbol{AX} = \boldsymbol{Y}$), independent of the number type and matrix structure. The matrix and number types are template parameters implemented by the template specialization techniques.

This is a definitive advantage of generic programming, the algorithm does not need to know the details of the data structures used as long a common interface is provided for each number or matrix type. Then, the numbers and matrix operations are the responsibility of the numbers and the matrix classes respectively. Consequently, the same algorithm works regardless of the type of the matrix or number provided.

In order to apply the concepts discussed so far in this paper, we modified a one-dimensional basin modeling software denominated GEOFEM—*Geological applications Of the Finite Element Method* [8] which was originally written in C, to produce C++ (GEOFEM++) in to perform interval and fuzzy operations. A specific EBE assembly operation was added to this software to obtain the global stiffness

matrix. We have adapted GEOFEM++ to perform Monte Carlo simulations with uniform, triangular, normal, and exponential density distributions.

6. Application to a Real, Multi-Layer Geological Case

In this section, we apply the techniques discussed in this paper and we compare the performance with more traditional methods to assess uncertainty. For the sake of simplicity, we discuss initially a very simple example to evaluate the algorithm efficiency in relation to the size of the mesh and the width of the interval numbers, after this, we applied the formulation to real data. So we performed four tests:

1. initial synthetic model,
2. increasing the number of elements,
3. increasing the interval numbers width,
4. test with real data.

For this discussion we consider the thermal conductivity uncertain.

6.1. Initial Synthetic Model

In Figure 4, we display a one-dimensional mesh representing the present-day column of sediments with 4 elements (layer) and 5 nodes (horizons). Table 3 shows the thermal conductivity values used in this test.

We calculated the evolution of this mesh over time, the results for a single node of the mesh at the present-day time are shown in Table 4. The value (15.86°C) is the result of a traditional deterministic simulation using real numbers (crisp solution) for the thermal conductivity (center value in Table 3). In the sequence, the Monte Carlo (MC) method was applied with 1000 experiments using a uniform distribution, and the results provide a range of uncertainty for the temperature between 15.31 to 16.41°C. For the uniform distribution, the average value is the same as the crisp solution. Note that an uncertainty of 13% to 17% in the thermal conductivity of the sediments induced a lower than 7% uncertainty in the temperature. The combinatorial method provides the range between 15.28 and 16.44, close to the MC method but with a little wider interval. Preconditioned Gaussian elimination and the Gauss-Seidel results are clearly overestimated, whereas Powell method generated a much tighter solution. Clearly, a poor selection of the interval solution method can provide inaccurate solutions. The EBE method provided a good solution close to the combinatorial method. This shows the advantages and limitations of the interval methods. In our opinion, the EBE method and MC method were able to assess the uncertainty accurately in this simple case.

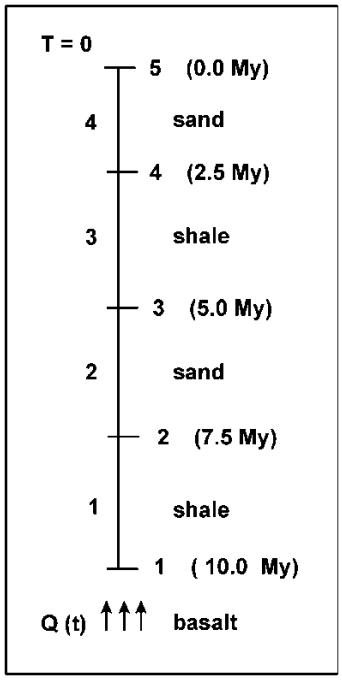

Figure 4. The elements in the mesh represent geological layers and the nodes the horizons. The respective age, in million of years (My) of each horizon, is shown on the right of the node numbers.

Table 3. Thermal conductivities values for shale and sandstone ($Wm^{-1}K^{-1}$).

Lithology	Interval Value
Shale	[1.45, 1.55]
Sandstone	[2.90, 3.10]

Table 4. Comparison among different solution methods for node 3 for the mesh displayed in Figure 4.

Method	Temperature (°C)
Crisp	15.86
Monte Carlo (MC)	[15.31, 15.86, 16.41]
Preconditioned Gauss Elimination	[12.38, 15.86, 21.80]
Preconditioned Gauss-Seidel	[10.77, 15.86, 26.35]
Combinatorial	[15.28, 15.86, 16.44]
Powell	[15.73, 15.86, 16.01]
EBE	[14.95, 15.86, 16.85]

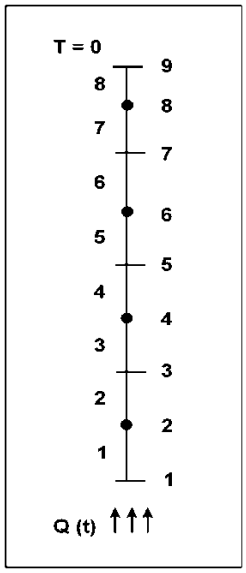

Figure 5. Mesh with 8 elements.

Table 5. Results for the node 5 of the mesh shown in Figure 5.

Method	Temperature (°C)
Crisp	15.66
Monte Carlo (MC)	[15.31, 15.66, 16.01]
Preconditioned Gauss Elimination	*Failed*
Preconditioned Gauss-Seidel	[4.07, 15.66, 37.89]
Combinatorial	[15.22, 15.66, 16.10]
Powell	[15.64, 15.66, 15.93]
EBE	[15.15, 15.66, 16.17]

6.2. INCREASING THE NUMBER OF ELEMENTS

In this experiment, we doubled the number of elements in the mesh as shown in Figure 5. The results for the node 5 are presented in Table 5.

When the number of the elements increases, the number of operations to invert the interval global stiffness matrix also increases, leading to potential problems for example, related to excessive overestimation. This can be verified in Table 5, especially for the Preconditioned Gauss-Seidel method. For this case, the preconditioned Gaussian elimination failed. This failure occurred due the large number of operations with interval number during the pivoting phase of the Gaussian elimination. The large number of operation tends to increase the width of interval number. This width may include zero in the range, making the interval division underdeter-

Table 6. Thermal conductivity for shale and sand (W/m °K).

Lithology	Interval Value
Shale	[1.40, 1.66]
Sandstone	[2.80, 3.20]

Table 7. Results increasing the thermal conductivity width of the shale and sand as shown in Table 6.

Method	Temperature (°C)
Crisp	15.86
Monte Carlo (MC)	*Failed*
Preconditioned Gauss Elimination	*Failed*
Preconditioned Gauss-Seidel	[14.68, 15.86, 16.92]
Combinatorial	*Failed*
Powell	[14.95, 15.86, 16.63]
EBE	[14.38, 15.86, 17.34]

mined. Similarly to the previous case, results of Powell's method were again too tight, and the MC and EBE methods provided good results.

6.3. Increasing the Interval Numbers Width

To evaluate the effect of a wider range of uncertainty, we used the new interval values of Table 6. The results for this experiment of the application of the selected methods are shown in Table 7. We used the same four-element mesh as displayed in Figure 4.

The increase in the range of uncertainty caused further deterioration in the quality of some of the solution methods. In this case, the preconditioned Gauss Elimination and Gauss- Seidel failed to converge. Powell's method converged to an incorrect result. EBE is the only interval method studied that provided results with good quality. It is interesting to note that the MC method resulted in slightly tighter result when compared with the solution hull. This result could be even tighter if one included a density distribution with a shape different from the box distribution we selected.

6.4. Multi-Layer Geological Example

As the last evaluation case, we applied the EBE, MC and Combinatorial methods to a well with real data. The stratigraphy is described in Table 8. There is 24 horizons and 23 layers, the Layer_23 is between the horizon_24 (depth = 7194 m, age = 135 My) and the horizon_23 (depth = 6500 m, age = 125 My), one source rock and one reservoir.

Table 8. The well's stratigraphy used in our analysis.

Layers	Depth (m)	Age (My)	Lithology	Interval Thermal Conductivity (W/m °K)
Layer_1	142.60	0.00	SHALE	[1.78, 2.18]
Layer_2	433.52	0.67	SHALE	[1.78, 2.18]
Layer_3	981.17	2.44	SHALE	[1.78, 2.18]
Layer_4	1197.99	13.20	SHALE	[1.78, 2.18]
Layer_5	1260.56	14.62	SHALE	[1.78, 2.18]
Layer_6	1362.75	23.55	SHALE	[1.78, 2.18]
Layer_7	1477.46	23.58	90SHALE10SAND	[1.88, 2.30]
Reservoir	1708.51	37.01	91SAND9SHALE	[2.72, 3.32]
Layer_9	2129.39	61.46	82SAND18SHALE	[2.62, 3.20]
Layer_10	2158.64	63.16	77SHALE23SAND	[2.02, 2.46]
Layer_11	2253.68	68.69	90SAND8SHALE2MARL	[1.87, 2.29]
Layer_12	2377.62	75.89	95SILT5SAND	[1.97, 2.41]
Layer_13	2408.27	77.67	77SAND17SHALE6SILT	[2.58, 3.16]
Layer_14	2484.35	82.09	75SAND23SHALE2SILT	[2.56, 3.12]
Layer_15	2905.23	84.11	70SAND20SILT10SHALE	[2.53, 3.09]
Layer_16	3494.79	85.08	50SILT40SHALE10SAND	[1.95, 2.39]
Layer_17	3861.44	85.69	SILT	[1.93, 2.35]
Layer_18	3884.26	96.00	68SHALE32SILT	[1.83, 2.23]
Layer_19	3951.24	110.92	65SAND23DOLOMITE12SILT	[3.83, 4.69]
Layer_20	3972.91	112.00	HALITA	[5.12, 6.26]
Layer_21	3979.57	113.00	CONGLOMERADE	[2.55, 3.11]
Source_Rock	5500.00	118.00	COQUINE	[2.64, 3.22]
Layer_23	6500.00	125.00	CONGLOMERADE	[2.55, 3.11]
	7194.00	135.00		

The number before the lithology composition (Lithology column) is the percentage of each lithology, for instance, 90SHALE10SAND means that in this layer there is 90% of shale and 10% of sand. The interval thermal conductivity was gotten by an error of 10% in the crisp values. For the Crisp method was used the midpoint of the interval thermal conductivity. The surface temperature is 18°C and the heat flux in the basement is 41.8 mW/m^2 for all ages.

For this analysis we assumed no variation in the paleobathymetry and sea-level over time. We built a finite element mesh with 69 elements, 3 elements per layer, to represent the stratigraphy listed in Table 8. For this modeling, we used the approach described in [9] and [10], which make use of a fully compacted coordinate system, to eliminate mesh deformation over time. Figure 6 summarizes the temperature calculation at the present-day time.

In this figure, we display the results for Crisp, Combinatorial (Comb), Monte Carlo (MC), and EBE methods. The other methods (Preconditioned Gauss Elimination, Preconditioned Gauss-Seidel and Powell) failed for this case. The uncertainty

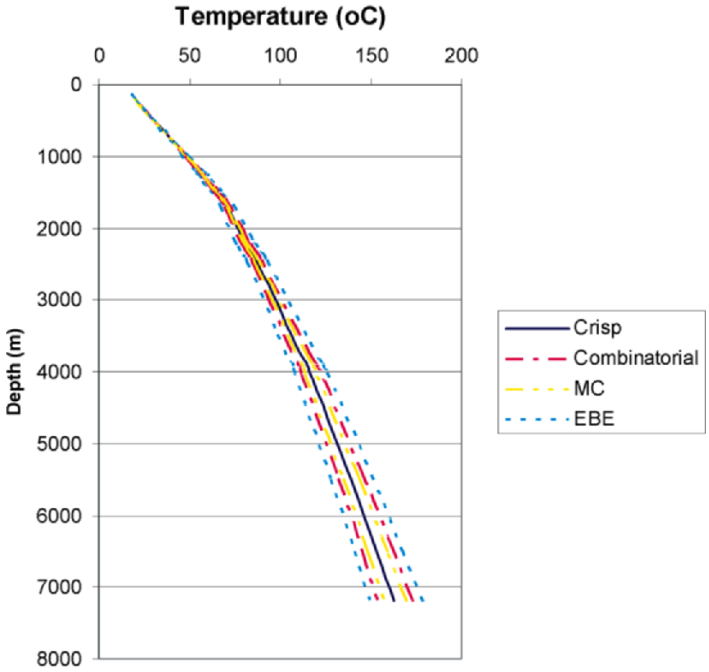

Figure 6. Temperature × depth for the data of Table 8.

Table 9. Temperature at depth 5500 m.

Method	Temperature (°C)
EBE	[151, 128]
Combinatorial	[132, 147]
Monte Carlo	[135, 144]
Crisp	139

increases with the depth due to the transient numerical solution. Note that, the EBE results were slightly outside the hull of the solution defined by the combinatorial method and the MC was between the EBE and Combinatorial results. Details can be seen in Table 9 which represents the values to the depth 5500 m. Enclosure algorithms [30] can obtain one narrower solution than EBE method. For the MC simulations, we used a uniform distribution of the thermal conductivity with 1000 scenarios and 15 histogram classes.

The EBE simulation took approximately 25 seconds and the MC took 150 minutes on an Intel P4 machine with 1.7GHZ and 1GB of RAM. The good quality of the EBE result was only achievable due to the EBE formulation that significantly reduces the number of interval operations.

7. Conclusions

In this work we evaluated the potential and limitations of an interval possibilistic approach to assess uncertainty in basin modeling. The interval arithmetic approach is an alternative to traditional probabilistic stochastic methodology. We extended the interval finite element EBE formulation to the transient heat transport equation. This formulation provided good results within the hull of possible solutions with a quality similar to the Monte Carlo method. However, the EBE formulation has the advantage of being able to perform the uncertainty analysis with a single simulation, requiring much less computational resources.

Here we compared the EBE formulation with the more traditional solutions for interval systems of equations and EBE has proved to be the most robust. The Preconditioned Gaussian elimination and Gauss-Seidel methods do not performed well with large meshes, either providing excessive overestimates or failing to converge. In addition, these methods also had problems to deal relatively wide numbers. Powell's method may produce incorrect or excessively tight results in basin modeling. The Combinatorial method, which provides the exact convex hull of the possible solutions, cannot be used in practical problems since it requires 2^n operations and becomes rapidly unviable when the number of interval variables grows.

The Monte Carlo method gives adequate results to the uncertainty analysis when there is sufficient statistical information about the variables. The MC method has the advantage of allow the analysis of multiple uncertain variables simultaneously without the need to change simulation applications. The major problem with the MC method is the computational cost.

The EBE with element overlap seems to be a viable alternative for one-dimensional basin modeling due to the quality of its results for the solution of transient problems. However further studies are necessary to analyze its possible application to multidimensional basin modeling using more parameters as interval numbers.

Acknowledgements

This paper has benefited greatly by the critically reviewing made by Andrew Conn/IBM and Anderson Moraes/Petrobras.

References

1. Burnett, D. S.: *Finite Element Analysis from Concepts to Applications*, Addison-Wesley, Whippany, 1987.
2. Deodato, S., Anile, A. M., and Privitera, G.: Implementing Fuzzy Arithmetic, *Fuzzy Sets and Systems* **72** (1995), pp. 239–250.
3. Hansen, E. R.: The Hull of Preconditioned Interval Linear Equations, *Reliable Computing* **6** (2) (2000), pp. 95–103.
4. Hanss, M.: On the Implementation of Fuzzy Arithmetical Operations for Engineering Problems, in: *Proceedings of the 8th International Conference of the North American Fuzzy Information Processing Society—NAFIPS 99*, New York, 1999, pp. 462–466.

5. Kaufman, A. and Gupta, M.: *Introduction to Fuzzy Arithmetic*, International Thomson Computer Press, 1991.
6. Kulpa, Z., Pownuk, A., and Skalna, I.: Analysis of Linear Mechanical Structures with Uncertainties by Means of Interval Methods, *Computer Assisted Mechanics and Engineering Sciences* **5** (1998), pp. 443–477.
7. McKenzie, D.: Some Remarks on the Development of Sedimentary Basins, *Earth Planet. Sci. Lett.* **40** (1978), pp. 25–32.
8. Mello, U. T.: *Thermal and Mechanical History of Sediments in Extensional Basins*, Ph.D. dissertation, Columbia University, 1994.
9. Mello, U. T. and Karner, G. D.: Development of Sediment Overpressure and Its Effect on Thermal Maturation: Application to the Gulf of Mexico Basin, *American Association of Petroleum Geologists Bulletin* **80** (9) (1996), pp. 1367–1396.
10. Mello, U. T., Karner, G. D., and Anderson, R. N.: A Physical Explanation for the Positioning of the Depth to the Top of Overpressure in Shale-Dominated Sequences in the Gulf Coast Basin, United States, *Journal of Geophysical Research* **99** (1994), pp. 2775–2789.
11. Mello, U. T. and Khabibrakhmanov, I.: On the Reusability and Numeric Efficiency of C++ Packages in Scientific Computing, in: *Proceeding of the ClusterWorld Conference and Expo, June 23–26, 2003 in San Jose, California*, 2003.
12. Moore, R. E.: *Interval Arithmetic and Automatic Error Analysis in Digital Computing*, Stanford University, 1962.
13. Muhanna, R., Ballarini, R., and Mullen, R.: Calculation of Stress Intensity Factors with Fuzzy Loading, in: *Proceedings of the 4th International Conference on Stochastic Structural Dynamics*, University of Notre Dame, Notre Dame, 1998, pp. 6–8.
14. Muhanna, R. L. and Mullen, R. L.: Development of Interval Based Methods for Fuzziness in Continuum Mechanics, in: *Proc. ISUMA-NAFIPS'95, September 17–20, 1995*, pp. 145–150.
15. Muhanna, R. L. and Mullen, R. L.: Formulation of Fuzzy Finite Element Methods for Mechanics Problems, *Computer-Aided Civil and Infrastructure Engineering* (previously *Microcomputers in Civil Engineering*) **14** (1999), pp. 107–117.
16. Muhanna, R. L. and Mullen, R. L.: Sharp Enclosure for Material Uncertainty in Solid and Structural Mechanics-Interval Based Approach, Part I, in: *Proceedings of the Eighth ASCE Joint Specialty Conference on Probabilistic Mechanics and Structural Reliability*, University of Notre Dame, Notre Dame, 2000, pp. 24–26.
17. Muhanna, R. L. and Mullen, R. L.: Treatment of Geometric Tolerances in Finite Element Analysis, *International Journal of Advanced Manufacturing Systems* **4** (1) (2001), pp. 143–162.
18. Muhanna, R. L. and Mullen, R. L.: Uncertainty in Mechanics Problems—Interval-Based Approach, *Journal of Engineering Mechanics, ASCE* **127** (6) (2001), pp. 557–566.
19. Mullen, R. L. and Muhanna, R. L.: Bounds of Structural Response for All Possible Loadings, *Journal of Structural Engineering, ASCE* **125** (1) (1999), pp. 98–106.
20. Mullen, R. L. and Muhanna, R. L.: Interval Based Finite Element Methods, in: Iliev, O. P. and Kaschiev, M. S. (eds), *Proceedings of the 4-th International Conference, NMA'98, Recent Advances in Numerical Methods and Applications II, Aug. 19–23*, World Scientific, 1998, pp. 362–371.
21. Mullen, R. L. and Muhanna, R. L.: Interval-Based Geometric and Material Uncertainty for Mechanics Problems, in: *Proceedings of the 13th ASCE Engineering Mechanics Division Conference*, The Johns Hopkins University, Baltimore, 1999, pp. 13–16.
22. Mullen, R. L. and Muhanna, R. L.: Structural Analysis with Fuzzy-Based Load Uncertainty, in: *Proc, 7th ASCE EMD/STD Joint Specialty Conference on Probabilistic Mechanics and Structural Reliability*, WPI, pp. 310–313.
23. Mullen, R. L. and Muhanna, R. L.: Sharp Interval Estimates for Finite Element Solutions with Fuzzy Material Properties, in: *Proceedings of the 14th ASCE Engineering Mechanics Conference*, The University of Texas at Austin, 2000, pp. 21–24.
24. Nakagiri, S. and Suzuki, K.: Finite Element Interval Analysis of External Loads Identified by Displacement Input Uncertainty, *Comput. Methods Appl. Mech. Engrg.* **168** (1999), pp. 63–72.
25. Neumaier, A.: *Interval Methods for Systems of Equations*, Cambridge University Press, New York, 1990.

26. Neumaier, A.: Overestimation in Linear Interval Equations, *SIAM J. Numerical Analysis* **24** (1) (1987), pp. 207–214.
27. Rao, S. S. and Berke, L.: Analysis of Uncertain Structural Systems Using Interval Analysis, *AIAA Journal* **35** (4) (1997), pp. 727–735.
28. Rao, S. S. and Li Chen: Numerical Solution of Fuzzy Linear Equations In Engineering Analysis, *Int. J. Numer. Meth. Eng.* **43** (1998), pp. 391–408.
29. Rao, S. S. and Sawyer, P.: Fuzzy Finite Element Approach for Analysis of Imprecisely Defined Systems, *AIAA Journal* **33** (12) (1995), pp. 2364–2370.
30. Rump, S. M.: Rigorous Sensitive Analysis for Systems of Linear and Nonlinear Equations, *Math. of Computations* **54** (90) (1990), pp. 721–736.

Appendix: Interval Arithmetic Notations and Operations

An interval number x is represented by:

$$x = [\underline{x}, \overline{x}],$$

where:

$\underline{x}$ = lower bound,
$\overline{x}$ = upper bound,
$\tilde{x}$ = is a real number that belongs to the interval number $x = [\underline{x}, \overline{x}]$,
$\grave{x}$ = is the real number midpoint of x.

$\operatorname{wid} x = \overline{x} - \underline{x}$ is the width of the interval number x.

Operations:

$$\begin{aligned}
x + y &= \lfloor \underline{x} + \underline{y},\ \overline{x} + \overline{y} \rfloor, \\
x - y &= \lfloor \underline{x} - \overline{y},\ \overline{x} - \underline{y} \rfloor, \\
x \times y &= \lfloor \min\{\underline{x}\underline{y}, \underline{x}\overline{y}, \overline{x}\underline{y}, \overline{x}\,\overline{y}\},\ \max\{\underline{x}\underline{y}, \underline{x}\overline{y}, \overline{x}\underline{y}, \overline{x}\,\overline{y}\} \rfloor, \\
\frac{1}{x} &= \left[\frac{1}{\overline{x}}, \frac{1}{\underline{x}}\right], \qquad \text{if } \underline{x} \times \overline{x} > 0.
\end{aligned}$$

Properties:

$$\begin{aligned}
x(y \pm z) &\subseteq xy \pm xz; \qquad x, y, z \in R, \\
x - y &\subseteq (x + z) - (y + z), \\
x / y &\subseteq (xz) / (yz), \\
x - x &\neq 0, \qquad 0 \in (x - x), \\
x / x &\neq 1, \qquad 1 \in x / x.
\end{aligned}$$

Note that when there is a repetition of a variable in a mathematical expression we get an overestimated result.